0023-6837/03/8309-1255$03.00/0
LABORATORY INVESTIGATION
Vol. 83, No. 9, p. 1255, 2003
Printed in U.S.A.
Copyright © 2003 by The United States and Canadian Academy of Pathology, Inc.

RESIDENT REVIEW SERIES

Identification of *CARS-ALK* Fusion in Primary and Metastatic Lesions of an Inflammatory Myofibroblastic Tumor

Larisa V. Debelenko, Diane C. Arthur, Svetlana D. Pack, Lee J. Helman, David S. Schrump, and Maria Tsokos

Laboratory of Pathology (LVD, DCA, MT), Pediatric Oncology Branch (LJH), and Thoracic Oncology Section, Surgery Branch (DSS), National Institutes of Health, National Cancer Institute, Bethesda, Laboratory of Immunopathology (SDP), National Institutes of Health, National Institute of Allergy and Infectious Diseases, Rockville, Maryland

SUMMARY: Inflammatory myofibroblastic tumor (IMT) is a rare childhood neoplasm. The natural history of this disease is poorly understood. Recently chromosomal rearrangements involving the anaplastic lymphoma kinase (*ALK*) gene have been implicated in this tumor. We have studied a case of ALK-positive soft tissue IMT showing clinical and morphologic features of malignancy. Interphase fluorescence in situ hybridization demonstrated *ALK* rearrangements in both primary and metastatic lesions. Rapid amplification of cDNA ends (5'RACE) identified cysteinyl-tRNA synthetase (*CARS*) gene fused to *ALK*, which predicts an in-frame chimeric protein with the preserved functional catalytic domain of ALK at the C terminus. Amplification and sequencing of tumor DNA confirmed the breakpoint at the genomic level. Restriction analysis of DNA from primary soft tissue and recurrent lung tumors showed identical patterns, indicating the same clonal origin of both lesions. Western blot analysis with C-terminus ALK antibody showed expression of an aberrantly sized chimeric protein of approximately 130 kd in tumor tissue. This is the second case of IMT demonstrating *CARS* as the *ALK* fusion partner, which confirms the recurring involvement of *ALK* in IMT by a common genetic mechanism. Moreover, identical clonality of separate lesions involving different sites supports metastasis in IMT. (*Lab Invest 2003, 83:1255–1265*).

Inflammatory myofibroblastic tumor (IMT) is a distinctive neoplasm that affects soft tissues and viscera and occurs predominantly in children and young adults (Coffin and Fletcher, 2002). In the past decade, IMT was recognized as a separate neoplastic entity within the spectrum of myofibroblastic lesions. The tumor is composed of myofibroblasts accompanied by a mixed inflammatory infiltrate and has a characteristic histology with three patterns represented in the same tumor: (a) myxoid, vascular, and inflammatory; (b) compact spindle cell; and (c) dense fibrotic (Coffin et al, 1995). In 1999 chromosomal rearrangements involving the anaplastic lymphoma kinase (*ALK*) locus on the short arm of chromosome 2 were identified in IMT (Griffin et al, 1999). These rearrangements result in expression and activation of the catalytic domain of the respective kinase and correlate with the positive immunohistochemical staining of tumor cells with C-terminal ALK antibodies (Coffin and Fletcher, 2002). Subsequently, ALK expression was detected in 40% to 60% of IMTs by immunohistochemistry (Cessna et al, 2002; Coffin et al, 2001; Cook et al, 2001). Molecular studies documenting *ALK* fusion partners in IMT are not numerous and have been limited to four reports thus far (Bridge et al, 2001; Cools et al, 2002; Lawrence et al, 2000; Ma et al, 2003). We present a case of soft tissue IMT with pulmonary metastases and prolonged progressive clinical course. We identify fusion involving *ALK* and cysteinyl-tRNA synthetase (*CARS*) genes in the tumor and show that this clonal aberration is present in both soft tissue primary and recurrent lung lesions, thus providing molecular evidence of the metastasis in IMT.

DOI: 10.1097/01.LAB.0000088856.49388.EA

Received July 7, 2003.
Address reprint requests to: Dr. Larisa V. Debelenko, Department of Pathology, Children's Hospital, 300 Longwood Avenue, Boston, Massachusetts 02115-5737. E-mail: Larisa.Debelenko@childrens.harvard.edu

Case Presentation

Clinical History. In 1991 a 10-year-old boy presented to the National Cancer Institute (NCI) for evaluation of a posterior cervical soft tissue mass detected by his mother. He had been in his usual state of good heath prior to this referral and specifically denied

fever, chills, malaise, pain, or antecedent trauma. Laboratory values including complete blood count, electrolytes, and liver chemistries were all within normal limits. Magnetic resonance (MR) and computed tomography (CT) scans revealed a soft tissue mass extending posteriorly along the vertebral spine from the level of the second cervical to the second thoracic vertebral body (Fig. 1A, 1 and 2). Needle biopsy was read as a spindle-cell sarcoma. The patient received vincristine, adriamycin, and cytoxan, alternating with VP16 and ifosfamide for 12 weeks without response. The mass was resected via posterior (laminectomy) approach 4 months after the initial diagnosis. All gross tumor was removed; however, microscopic foci of tumor cells were noted in deep tissues adjacent to C5-C6 transverse processes. The patient received

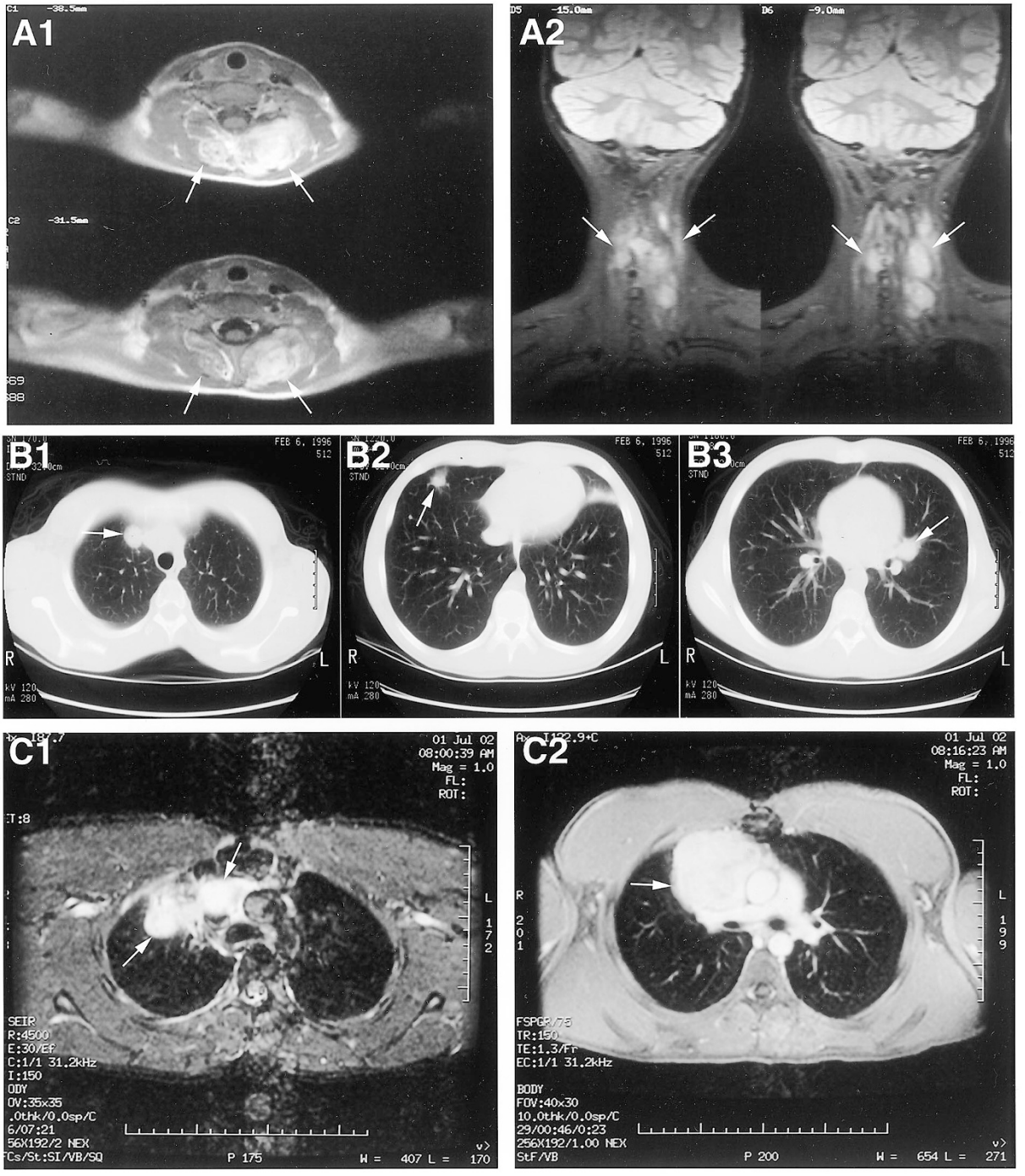

Figure 1.

(A, 1 and 2) Magnetic resonance (MR) images revealing posterior cervical tumor (*arrows*) at initial presentation in 1991. (B, 1 to 3) Computed tomography images revealing lesions in the right-upper lobe (B1), right-middle lobe (B2), and left hilum (B3) prior to resection in 1996. All three discrete nodules are confined to pulmonary parenchyma. (C1) Two MR scan images revealing extensive recurrence in right lung and anterior mediastinum. The mass appears to have arisen from two pulmonary nodules (C1) that coalesced, extending to the anterior chest wall, and encasing the superior vena cava (C2).

adjuvant external beam radiation therapy (6800 cGy) to the neck and upper chest. Serial CT and MR scans from 1992 to 1996 revealed slowly evolving nodules in the parenchyma of the right lung (Fig. 1B, 1 and 2), as well as the left pulmonary hilum (Fig. 1B3). No local recurrence was noted. The patient remained asymptomatic. In 1996, the patient underwent median sternotomy, and the nodule in the right-upper lobe (Fig. 1B1) as well as the right-middle lobe nodule (Fig. 1B2) were removed. Pathologic analysis of the resected tissues showed IMT. During the ensuing years, the patient remained in good health. Serial imaging studies revealed recurrence of tumor within the right-upper lobe, which eventually extended to the apex of the right hemithorax anteriorly, and enveloped the superior vena cava from the level of the innominate veins to the cavo-atrial junction (Fig. 1C, 1 and 2); the previously noted left hilar mass remained relatively stable. In 2002 the patient underwent redo-median sternotomy with right-upper lobectomy, partial right-middle lobectomy, and en bloc resection with reconstruction of the superior vena cava. All gross disease was removed; however, microscopic foci of tumor cells were observed at the apical margins of resection. The patient was in excellent health 1 year following aggressive resection of the pulmonary/mediastinal recurrence. CT scans revealed no disease in the right hemithorax or superior mediastinum. The left hilar mass has increased approximately 20% during the past year.

Pathology Findings. The primary paraspinal mass (needle biopsy in 1991, surgical removal in 1992) measured 10.5 cm in greatest dimension. Histologically the tumor was predominantly composed of a compact proliferation of large spindle cells growing in a fascicular pattern (Fig. 2A). The tumor cells had pale eosinophilic cytoplasm and large vesicular nuclei with prominent nucleoli, and focally resembled ganglion cells (Fig. 2B). Although cellular atypia, variation in nuclear size and shape, and rare multinucleated cells were present, no significant pleomorphism was seen. Neither mitosis nor areas of necrosis were identified. A rather scant but notable mixed inflammatory infiltrate was present. Along the cellular areas, foci of dense scar-like fibrosis were seen (Fig. 2A). The fascicles of spindle cells infiltrated surrounding striated muscles, and several surgical margins remained positive. Electron microscopy demonstrated the myofibroblastic differentiation of the lesional cells: elongated shape, taped and "accordion-like" nuclei, abundant cytoplasm with well-developed rough endoplasmic reticulum, and thin filaments, with intercalated dense bodies and subplasmalemmal attachment plaques (Fig. 2C). Upon re-review of the case, the tumor was reclassified as an IMT.

Open biopsies of two separate peripheral lung nodules performed 5 years after the original presentation showed morphology similar to that of the paraspinal mass. The lesions had a stellate shape due to the perivascular and septal growth pattern. The mixed inflammatory infiltrate was, however, more pronounced than in the primary tumor, and at the periphery of the nodules it was dense and severe (Fig. 2D).

The lung mass removed in 2002 (right-upper lobectomy) measured 7 cm and showed the typical three-component histology of IMT, consisting of compact spindle cell, myxoid edematous, and dense scar-like patterns (Coffin et al, 1995). Immunohistochemistry showed strong cytoplasmic staining for ALK (Fig. 2E). In keeping with the myofibroblastic differentiation, the cells were positive for vimentin and smooth muscle actin (antigene 1A4). The HHF-45, S100, CD34, CD31, cytokeratin AE1/3, EMA, CD30, and myogenin (MYF-4) immunostains were negative. A subset of tumor cells was positive for C-kit ($<$ 50%), p53 (10%), and Ki67 (10%).

All lesions, primary and metastatic, showed various degrees of cellularity and cellular atypia; however, we did not observe any cytomorphologic transformation over the period of 10 years. As in the primary paraspinal tumor, no mitotic activity was identified in the lung nodules, and $<$ 10% of cells stained for Ki67. However, some histologic features of malignancy were observed in the lung mass (2002), including a few microscopic foci of tumor necrosis (Fig. 2F), and bronchial and vascular invasion (Fig. 2, G and H).

Cytogenetics Findings. Eight suspension and three monolayer cultures were established from the lung tumor (2002) for metaphase and interphase cytogenetics studies. The mitotic index of the tumor was very low in all of the cultures. A total of 29 metaphase cells were found on 27 slides for G-banded analysis. No clonal numerical or structural chromosome abnormalities were detected.

Interphase fluorescence in situ hybridization (FISH) was also performed on the lung tumor (2002) using the LSI *ALK* Dual Color, Break Apart Rearrangement Probe (Vysis, Inc.). FISH revealed that a majority (90%) of the nuclei were small and round, and a minority (10%) were large, often oblong or horseshoe-shaped. Of 340 small nuclei scored, 333 (98%) showed no rearrangement of the *ALK* gene (Fig. 3A1). The remaining seven small nuclei (2%) had balanced rearrangement of one of the two *ALK* genes. A total of 146 large nuclei were scored. Fifty-nine percent of the large nuclei had two copies of *ALK*; only 1% of these had rearrangement of one of the *ALK* genes. The remaining 41% had multiple copies of *ALK*, and 76% of these had rearrangements. Although a few of the rearrangements were balanced (Fig. 3A2), most were unbalanced (Fig. 3A3), with loss of the 5' (centromeric) portion of *ALK*, and extra copies of the 3' (telomeric, presumably translocated) portion. Interphase FISH was also performed on touch preparations from frozen primary tumor resected in 1991. Forty-seven percent of the evaluable nuclei had unbalanced *ALK* rearrangements, and all nuclei with rearrangements of *ALK* were large (Fig. 3B).

Molecular Findings. To identify the *ALK* fusion partner, the initial 5'RACE run was performed on the lung tumor (2002) RNA. Because no products were detected on ethidium bromide staining, nested PCR of the diluted 5'RACE products was carried out, which

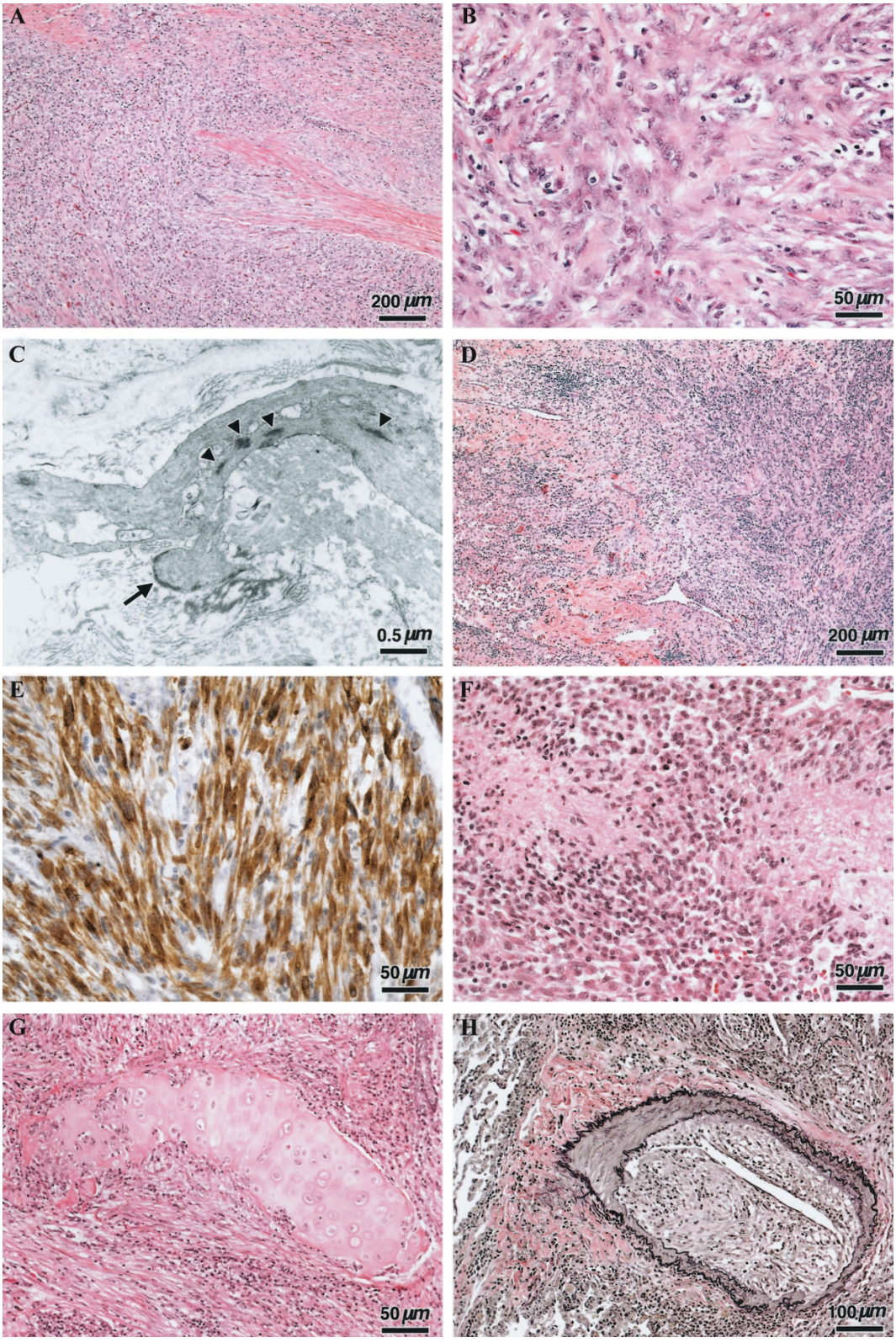

Figure 2.

(A and B) Primary posterior cervical tumor, 1991 (See also Fig. 1A). (A) Cellular areas of tumor growing in fascicular pattern are intermixed with scar-like fibrosis (hematoxylin eosin). (B) Large myofibroblastic cells with vesicular nuclei and prominent nucleoli are embedded in collagenous matrix and intermixed with inflammatory cells (hematoxylin eosin). (C) Peripheral portion of the myofibroblast shows abundant intermediate filaments, dense bodies (*arrowheads*), and attachment plaques (*arrow*) (electron microscopy). (D) Right-middle lobe nodule, 1996 (See also Fig. 1B2). The lesion shows scar-like fibrosis as well as cellular areas. Prominent inflammatory infiltrate is present at the periphery (hematoxylin eosin). (E to H) Recurrent metastatic central lung mass, 2002 (See also Fig. 1C2). (E) Strong cytoplasmic staining for anaplastic lymphoma kinase (immunohistochemistry). (F) Microscopic areas of tumor necrosis (hematoxylin eosin). (G) Tumor infiltrating small bronchus (hematoxylin eosin). (H) Tumor invading into a small-to-intermediate caliber intrapulmonary artery at the periphery of the mass (Van Gieson stain).

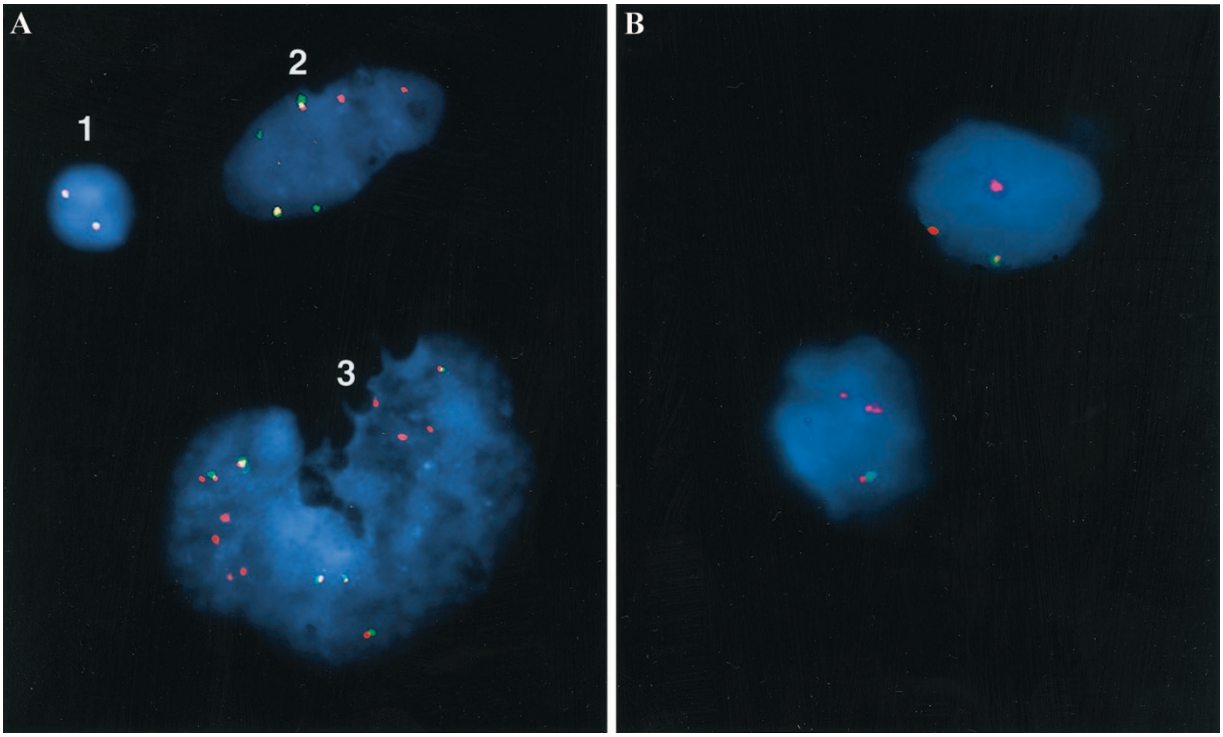

Figure 3.

Interphase fluorescence in situ hybridization with the LSI *ALK* Dual Color, Break Apart Rearrangement Probe (Vysis, Inc.). (A) Lung mass resected in 2002 revealing (1) small nucleus with no rearrangement of *ALK*, (2) oblong nucleus with two normal copies and two balanced rearrangements of *ALK*, and (3) large horseshoe-like nucleus with multiple normal copies and unbalanced rearrangements of *ALK* signified by loss of the 5' centromeric (green signal) and extra copies of the 3' telomeric (red signal) portions of this gene. (B) Primary tumor resected in 1991 showing unbalanced *ALK* rearrangements (loss of 5' and extra copy of 3' portions) in two large nuclei.

yielded strong bands of approximately 350 bp, 400 bp, and 1300 bp. These PCR products were cloned, and the inserts from the selected clones were sequenced. Sequence analysis of four independent clones from two different experiments yielded identical uninterrupted sequences containing a portion of ALK cDNA sequence preceded by at least 212 bp of a non-ALK sequence. BLASTN (basic local alignment search tool nucleotide) analysis revealed the non-ALK sequence to be 100% identical to the CARS mRNA (NM_139273), (Fig. 4A). The breakpoint is identical to the one previously reported in the CARS-ALK fusion (Cools et al, 2002).

To confirm the fusion at the genomic level, DNA extracted from the same lung tumor (2002) was amplified with two primers located in the intronic sequences flanking the predicted fused exons of *CARS* (exon 17, NM_001751) and *ALK* (exon 15, NM_004304). This amplified a 1760-bp fragment, the sequence analysis of which showed that first 1271 nucleotides from the 5' end represented the *CARS* genomic sequence, while 491 nucleotides in the 3'portion originated from the *ALK* genomic sequence. Two nucleotides (AT) located at the genomic junction overlap in the sequences of both genes and might originate from either *CARS* or *ALK* (Fig. 4B).

To define whether the same chimeric gene was present in the primary tumor, a short intronic fragment encompassing the breakpoint was amplified and showed products of the expected size (155 bp) in both primary (from 1991) and metastatic lung (from 2002) tumors. Restriction digestion with *Dra*II, the site located in the amplified 155-bp fragment, showed identical and predicted patterns in both lesions (Fig. 5). The data confirm that the chromosomal rearrangement involving *ALK* is the primary event and demonstrate the same clonal origin of the primary and recurrent tumors.

To confirm the expression of the chimeric protein in the tumor tissue, Western blot analysis was performed using protein extracted from the snap-frozen tumor tissue (from 2002). Immunoblotting with the rat polyclonal antibody raised against aminoacids 1359 to 1446 of human ALK showed a prominent band of approximately 130 kd, the molecular weight corresponding to the predicted CARS-ALK chimera (Fig. 6). The data confirm the strong expression of the fusion protein with the preserved ALK catalytic domain at the C terminus.

Review of the Literature

Terminology and Prognosis. The term IMT emerged in 1990 from the study of a series of lung lesions composed of admixed spindle and inflammatory cells (Pettinato et al, 1990). The authors demonstrated the myofibroblastic differentiation of the spindle cells and suggested the term IMT instead of the previously used "inflammatory pseudotumor" or "plasma cell granuloma/histiocytoma" (Spencer, 1984). Subsequently, IMT

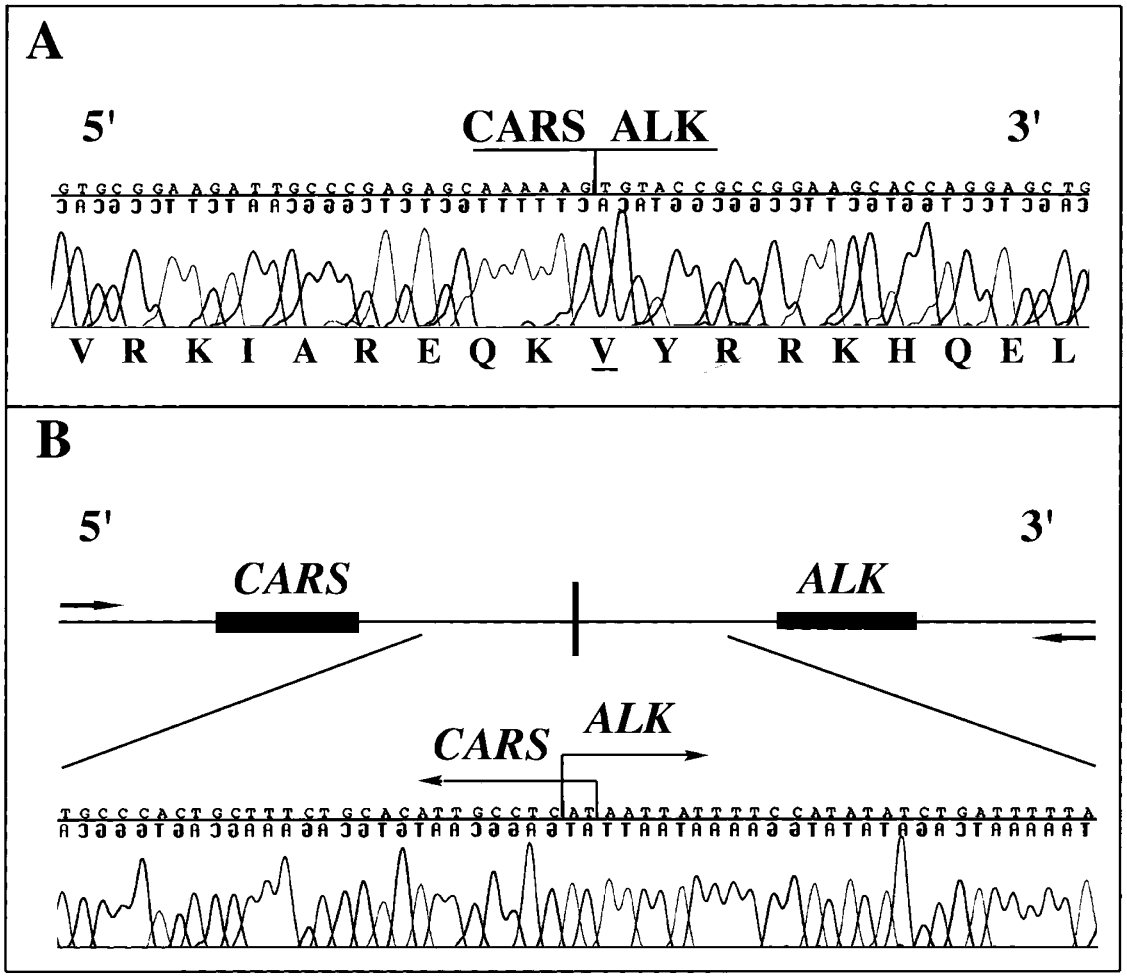

Figure 4.

Fusion transcript and genomic DNA sequencing of the breakpoint in recurrent metastatic lung inflammatory myofibroblastic tumor (from 2002). (A) Chromatogram showing the sequence of CARS-ALK fusion transcript at the breakpoint. The CARS sequence at the 5' portion of the transcript (left) is followed by the ALK sequence at the 3' portion (right). Lower line shows the transcription of the fusion. Note the last nucleotide of the CARS portion of the sequence (G) contributes to the GTG triplet encoding Valine (*underlined*), maintaining the in-frame translation of the ALK catalytic domain at the C terminus of the predicted chimeric protein. (B) The scheme and chromatogram showing the genomic breakpoint of the hybrid *CARS-ALK* gene. The genomic DNA was amplified with the primers located in intronic sequences flanking the fused exons of both genes (*thick arrows*). The resulting 1760-bp fragment was cloned and sequenced. The chromatogram shows the portion of the intronic hybrid sequence in the proximity of the breakpoint. Two nucleotides at the intronic junction (AT) are identical in both fused genes and might be contributed by either of them.

was described in a variety of extra-pulmonary sites. IMT was originally viewed as a reactive tumor-like lesion because of its low-grade histology, pronounced inflammatory component, and benign clinical course in most of the cases. However, demonstration of invasion, recurrence and metastasis, as well as identification of clonal cytogenetic aberrations in subsets of the lesions, have led to the reappraisal of IMT as a neoplastic disease (Coffin et al, 1998a, 1998b, 2001; Donner et al, 1996; Meis-Kindblom et al, 1998). A group of tumors with the predominantly mesenteric location described under the term "inflammatory fibrosarcoma" (Meis et al, 1991) was later interpreted as a more aggressive part of the IMT spectrum (Coffin et al, 1998a; Meis-Kindblom et al, 1998). The recurrence rate of IMT is approximately 25%, the multifocality is frequent, but the metastatic rate is low and ranges from $<$ 5% to 11% in different series (Coffin et al, 1995, 2001; Meis et al, 1991). Recently several single case reports additionally documented metastasis in IMT (Dishop et al, 2003; Lacoste-Collin et al, 2003; Trojan et al, 2001). However, the higher metastatic rate has not been confirmed in larger series. Therefore, the IMT is currently defined as an intermediate tumor with the potential to recur but with rare metastatic potential (Coffin and Fletcher, 2002; Kempson, 2001).

Reliable features to predict the clinical outcome of IMT have not been established (Coffin et al, 1998a; Meis-Kindblom et al, 1998). Some authors suggest that deep location, large size, and young age correlate with the recurrent disease (Meis-Kindblom et al, 1998). It was also shown that combination of atypia, ganglion-like cells, p53 expression, and aneuploidy may be useful in delineation of more aggressive IMTs (Hussong et al, 1999). The influence of ALK status has been studied, and though not statistically significant, the results indicated that ALK-positive IMTs had a

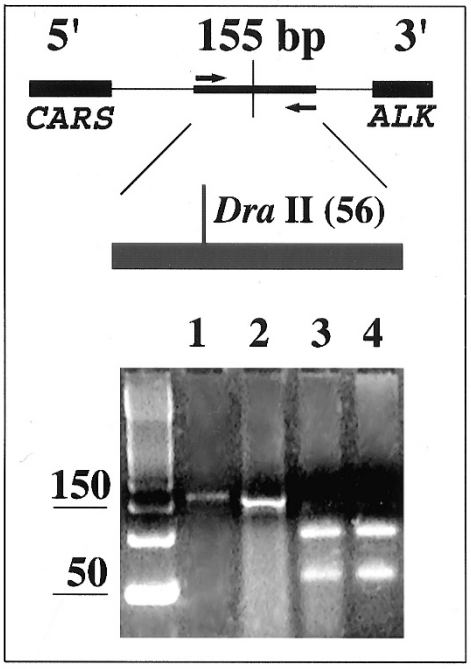

Figure 5.
Restriction digest of genomic fusion in primary (from 1991) and recurrent metastatic lung (from 2002) tumors. Genomic DNA from the primary spinal mass and recurrent metastatic lung tumor was amplified with the primers flanking the intronic junction (*arrows*) and analyzed on a 4% agarose gel (bottom panel). PCR products of expected size (155 bp) were observed in both samples (Lane 1, primary spinal mass; Lane 2, recurrent lung tumor). After the digestion with *Dra*II, identical and expected restriction patterns were seen in both primary (Lane 3) and recurrent metastatic (Lane 4) lesions.

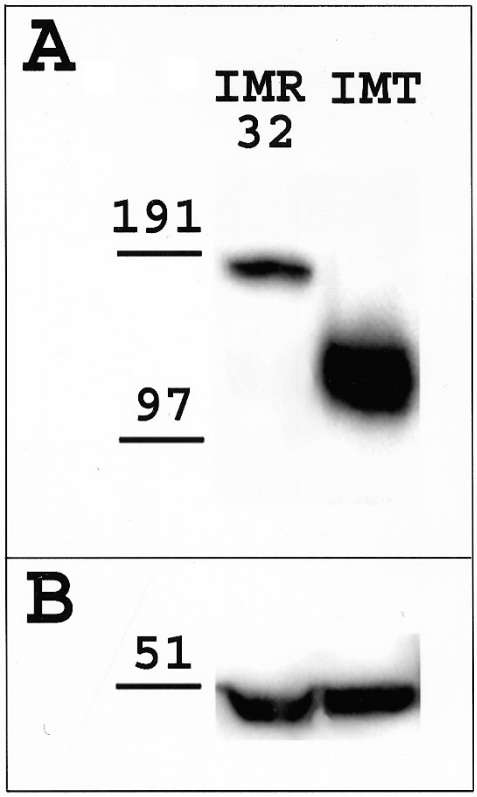

Figure 6.
Western blot analysis of the recurrent metastatic tumor with a rat polyclonal antibody raised against aminoacids 1359 to 1446 at the C terminus of human ALK. (A) Control neuroblastoma cell line IMR32 shows a single band of approximately 180 kd, corresponding to the full length anaplastic lymphoma kinase (ALK). The inflammatory myofibroblastic lung tumor (from 2002) shows an intense band, approximately 130 kd, indicating the aberrantly sized chimeric protein with the preserved C terminus of ALK. (B) Sample loading control with the α-tubulin antibody.

male predilection, affected younger individuals, and showed a higher recurrence rate (Coffin et al, 2001).

The case analyzed here presented in a male at a relatively young age (10 years) as a large mass (10.5 cm) located in the deep paraspinal soft tissue. Initial pathology showed cellular atypia and ganglion-like cells. The tumor was ALK-positive, and cytogenetics revealed the *ALK* rearrangement. All of the above features have been proposed to be associated with a more aggressive clinical course and recurrence. Pulmonary nodules were detected by imaging 1 year after the treatment of primary tumor, and the metastatic nature of the pulmonary recurrence was verified by a finding of the same *CARS-ALK* fusion in both lesions from distant sites.

ALK Involvement in IMT and CARS-ALK Fusion. Early cytogenetics studies of IMTs showed various complex karyotypic abnormalities, frequently involving the short arm of chromosome 2 (Snyder et al, 1995; Su et al, 1998; Treissman et al, 1994). In 1999 a specific clonal rearrangement involving the *ALK* locus in chromosome band 2p23 was demonstrated in two cases of IMT (Griffin et al, 1999). The *ALK* gene encodes for a receptor tyrosine kinase, which belongs to the insulin receptor subfamily. It was identified in 1994 as a fusion partner of a hybrid gene cloned from the anaplastic large cell lymphoma (Morris et al, 1994). A total of 11 apparently unrelated *ALK* fusion partners have been identified in lymphoma and IMT to date (Bridge et al, 2001; Cools et al, 2002; Hernandez et al, 1999; Lamant et al, 1999, 2003; Lawrence et al, 2000; Ma et al, 2003; Morris et al, 1994, 2001; Siebert et al, 1999; Tort et al, 2001), and one of them, *CARS*, was demonstrated previously only once in a prenatal case of IMT (Cools et al, 2002).

Besides *CARS*, four other *ALK* fusion partners were documented in IMT, including *TPM3* and *TPM4* (Lawrence et al, 2000), clathrin heavy chain (*CLTC*) (Bridge et al, 2001), and *RANBP2* (Ma et al, 2003). Although CLTC-ALK and tropomyosin-ALK were also detected in lymphoma (De Paepe et al, 2003; Gascoyne et al, 2003; Lamant et al, 1999; Siebert et al, 1999), RANBP2-ALK and CARS-ALK appear more prevalent in IMT, as they have so far been detected exclusively in this tumor type. Although multiple translocation partners are fused to *ALK*, each translocation product retains the last 563 amino acids of the kinase with its catalytic domain (Morris et al, 2001). Apparently unrelated, diverse *ALK* fusion partners are ubiquitously expressed and share the ability (known or predicted) to mediate homo-oligomerization of the respective fusion proteins, mimicking the kinase activation normally mediated by a ligand binding to the receptor (Rodrigues et al, 1994; Bischof et al, 1997). This

persistent and ectopic ALK activation is thought to be a key transforming event, and phosphorylation and transforming abilities of several ALK hybrids have been demonstrated (Bischof et al, 1997; Hernandez et al, 2002; Lawrence et al, 2000).

The predicted CARS-ALK transcript contains an open reading frame of 3507 nucleotides, which encode for a 1169-aminoacid chimeric protein. The first 606 amino acids of the chimera represent 81% of the CARS sequence including its N terminus. CARS catalyzes the addition of cysteine to its cognate RNA and is ubiquitously expressed. Two transcript variants of CARS cDNA were isolated, resulting from the alternative splicing in the 3'coding region (Davidson et al, 2001). This alternative splicing occurs downstream of the breakpoint identified in IMT and does not affect the sequence of the CARS-ALK chimeric protein. Comparison of molecular weights of the human CARS determined by gel filtration chromatography and SDS-PAGE suggested that the enzyme exists as multimers, most likely dimers (Davidson et al, 2001). Thus, *CARS* likely contributes to the neoplastic transformation by lending an active promoter and mediating the homo-oligomerization of the chimeric product, which activates ALK similar to other ALK fusions (Morris et al, 2001). Our finding of cytoplasmic immunostaining for ALK suggests that the distribution of the ALK-CARS chimera within the cell is probably determined by its CARS portion, in keeping with the normal location of aminoacyl-tRNA synthetases predominantly in the cytoplasm (Popenko et al, 1993).

The *CARS* gene is mapped to chromosome band 11p15.5, the region containing the imprinted domain and tumor suppressor genes lost in Wilms tumor and embryonal rhabdomyosarcoma (Hu et al, 1997; Reid et al, 1997). Chromosomal rearrangement underlying the *CARS-ALK* fusion might affect the transcription of other genes in the proximity of the breakpoint on chromosome 11p15.5, which may independently contribute to a relatively aggressive tumor behavior. The IMT case with the *CARS-ALK* fusion reported previously (Cools et al, 2002) showed a complex translocation involving chromosome band 11p15 and unusual clinical presentation, being diagnosed in utero as a relatively large mass located in the paravertebral soft tissue of the male fetus at 32 weeks of gestation (Sirvent et al, 2001).

Conclusion

We report here for the first time identical clonal ALK rearrangements detected in separate lesions of an IMT, which supports the metastatic potential of this tumor. Our retrospective clinical analysis also demonstrates that IMT can follow an insidious protracted course (over 10 years), in the presence of metastatic disease. Ours is the second tumor case documenting *CARS* as the *ALK* fusion partner; both IMTs with CARS-ALK fusion variant affected young men and had paraspinal soft tissue location. Additional molecular studies combined with clinico-pathological analysis might clarify whether *ALK* involvement or particular ALK fusion variants can discriminate subsets of IMTs with similar characteristics and prognosis.

Materials and Methods

The patient has been enrolled on NCI IRB-approved protocol 86-C-0169 for more than a decade. All treatments, procedures, and laboratory studies have been performed in accord with the National Institues of Health Human Subjects Research policies and with appropriate signed informed consent.

Pathology

Pathology reports and sections of the primary and recurrent lesions were reviewed by two pathologists (MT, LVD). Immunohistochemistry for ALK (Zymmed); SMA, CD31, CD34, EMA, p53, and Ki67/MIB1 (Daco); CD30, C-kit, and MYF-4/myogenin (Novocastra/Vector Laboratories); S100 (Biogenics); cytokeratin AE1/3 (Boehringer and Mannheim); and actin/HHF-45 (ENZO Diagnostics) was performed using standard laboratory protocols and automated processing (Ventana).

Cytogenetics

Fresh tumor resected in 2002 was processed for G-banded metaphase chromosome and interphase FISH analyses using routine laboratory procedures. A 1-cm^3 piece of cellular soft tissue was finely minced and used to set up two suspension and three monolayer cultures. A more fibrotic 3-cm^3 piece was minced, exposed to 0.8% type 1A-S collagenase for 2 hours at 37° C, and used to set up six suspension cultures. Cell suspensions were cultured in duplicate, in RPMI 1640 medium supplemented with 17% fetal bovine serum (Gibco), L-glutamine, and penicillin/streptomycin, for 24, 72, 96, and 120 hours. Triplicate monolayer cultures were established in Alpha Minimal Essential Medium with supplements as above; the medium was changed on Day 4, and cultures were harvested on Days 8, 11, and 12. Duplicate suspension cultures were harvested by exposing the cells to 0.07 μg/ml Colcemid for 2 or 4 hours, respectively, and then to 0.075 M KCl for 12 minutes. Cell pellets were fixed twice with 3:1 methanol to glacial acetic acid. Monolayer cultures were harvested and fixed similarly, with trypsinization (5 μg/ml trypsin-EDTA) following 4-hour exposure to Colcemid. For G-banded chromosome analysis, the cell pellets were fixed a third time, dropped onto glass slides, and stained with Wright stain. All metaphase cells present were fully analyzed at the 400 to 550 band level of resolution, and eight digital images were captured and karyotyped using a Cytovision system (Applied Imaging, Santa Clara, California). Karyotypes were designated according to the International System for Human Cytogenetic Nomenclature, 1995 (Mitelman, 1995). For interphase FISH, the same cell pellets as mentioned above were used to drop slides that were hybridized with the LSI *ALK* Dual Color, Break Apart Rearrangement Probe (Vysis, Inc.). Interphase nuclei were scored for unrearranged (red and green signals

overlapping or close together) and rearranged (solitary red or green signals) *ALK* using a 4',6-diamidino-2-phenylindole-2-HCl (DAPI) counter stain and a Zeiss fluorescence microscope with a Chroma filter set that includes DAPI, fluorescein isothiocyanate, and rhodamine filters. Digital images were captured on Cytovision. Interphase FISH was subsequently performed on touch preparations of frozen primary tumor resected in 1991. Cells were fixed with 70% ethanol, dehydrated, hybridized with the Vysis LSI *ALK* Probe, and analyzed as mentioned above.

RNA isolation, c-DNA synthesis, and 5'RACE

RNA was isolated from frozen lung tumor (from 2002) using the TRIzol Reagent (Invitrogen). cDNA was synthesized from 2 μg of total RNA per reaction using Superscript First Strand Synthesis System (Invitrogen) and two primers located in the ALK transcript (5'TTCAGGCAGCGTCTTCACAG (Maes et al, 2001) and 5'AGGTCTTGCCAGCAAAGCAGTAGTT (Lawrence et al, 2000). Further, 5'RACE (Invitrogen) was performed with the abridged anchor primer and two ALK-specific primers (5'AGGTCTTGCCAGCAAAGCAGTAGTT and 5'CGGAGCTTGCTCAGCTTGTACTC, respectively [Lawrence et al, 2000]), followed by reamplification with the abridged universal amplification primer and two ALK-specific primers (5'CGGAGCTTGCTCAGCTTGTACTC and 5'AGCTCCATCTGCATGGCTTG [Cools et al, 2002], respectively).

Sequence Analysis

5'RACE PCR products were cloned into the pCTR.1 TOPO vector (Invitrogen). Plasmids from 10 colonies from two independent reactions were analyzed for the presence of the insert, after restriction digestion with *Eco*RI (Promega). Selected plasmids with inserts were sequenced using vector primers. Sequences were analyzed using the BLASTN algorithm (National Center for Biotechnology Information).

DNA Isolation, Amplification, and Restriction Digest Analysis

Genomic DNA was extracted from both primary (from 1991) and recurrent (from 2002) tumor samples as previously described (Debelenko et al, 1997). To identify the genomic breakpoint, DNA from the recurrent tumor (2002) was amplified with primers located in intronic sequences flanking the fused exons of *CARS* (5'ACTGAGCTATTATTCTGTTA) and *ALK* (5'TCTGCGGTGCTGTGATAACATT). The amplified fragment was cloned, sequenced, and analyzed as described above. The second set of intronic primers was designed to amplify a shorter (155-bp) fragment encompassing the breakpoint. These were 5'AATTGGTGAGTAACAGCACAGCT (from the *CARS* intronic sequence) and 5'TGTCTTTAATTGAAGCATGAT (from the *ALK* intronic sequence). DNA from both primary (1991) and recurrent (2002) tumors was amplified with the second set of the intronic primers and analyzed on a 4% agarose gel, before and after restriction digestion with *Dra*II (Promega), a site located in the amplified 155-bp fragment.

Western Blotting

Protein was extracted from frozen lung tumor (from 2002) by grinding in the ice-cold radioimmunoprecipitation assay buffer (Bischof et al, 1997), resolved on a reducing 10% BIS-TRIS polyacrylamide gel (Invitrogen) and transferred to polyvinylidene difluoride membrane (Amersham Pharmacia Biotech). The membrane was blocked with $\times$1 casein solution (Vector Laboratories) and incubated with the rabbit polyclonal antibody raised against aminoacids 1359 to 1446 of human ALK (Zymed) at a dilution 1:1000 at 4° C, overnight. Following incubation with the secondary antirabbit IgG-HRP (Santa Crus Biotechnology), the membrane was developed using the electrochemiluminescence kit (Amersham Pharmacia Biotech). The neuroblastoma cell line IMR32, with known full length ALK expression (Lamant et al, 2000), was used as a positive control.

Acknowledgements

The authors gratefully acknowledge the technical expertise of April Tos, CLSp(CG), and Shannon Skarshaug, MS, in the performance of the cytogenetic analyses.

References

Bischof D, Pulford K, Mason DY, and Morris SW (1997). Role of the nucleophosmin (NPM) portion of the non-Hodgkin's lymphoma-associated NPM-anaplastic lymphoma kinase fusion protein in oncogenesis. Mol Cell Biol 17:2312–2325.

Bridge JA, Kanamori M, Ma Z, Pickering D, Hill DA, Lydiatt W, Lui MY, Colleoni GW, Antonescu CR, Ladanyi M, and Morris EW (2001). Fusion of the ALK gene to the clathrin heavy chain gene, CLTC, in inflammatory myofibroblastic tumor Am J Pathol 159:411–415.

Cessna MH, Zhou H, Sanger WG, Perkins SL, Tripp S, Pickering D, Daines C, and Coffin CM (2002). Expression of ALK1 and p80 in inflammatory myofibroblastic tumor and its mesenchymal mimics: A study of 135 cases. Mod Pathol 15:931–938.

Coffin CM and Fletcher JA (2002). Inflammatory myofibroblastic tumor. In: Fletcher CDM, Unni KK, and Mertens F, editors. Pathology and genetics of tumors of soft tissue and bone. Lyon: IARC Press, 91–93.

Coffin CM, Dehner LP, and Meis-Kindblom JM (1998a). Inflammatory myofibroblastic tumor, inflammatory fibrosarcoma, and related lesions: A historical review with differential diagnostic considerations. Semin Diagn Pathol 15:102–110.

Coffin CM, Humphrey PA, and Dehner LP (1998b). Extrapulmonary myofibroblastic tumor: A clinical and pathological survey. Semin Diagn Pathol 15:85–101.

Coffin CM, Patel A, Perkins S, Elenitoba-Johnson KS, Perlman E, and Griffin CA (2001). ALK1 and p80 expression and chromosomal rearrangements involving 2p23 in inflammatory myofibroblastic tumor. Mod Pathol 14:569–576.

Coffin CM, Watterson J, Priest JR, and Dehner LP (1995). Extrapulmonary inflammatory myofibroblastic tumor (inflammatory pseudotumor): A clinicopathologic and immunohistochemical study of 84 cases. Am J Surg Pathol 19:859–872.

Cook JR, Dehner LP, Collins MH, Ma Z, Morris SW, Coffin CM, and Hill DA (2001). Anaplastic lymphoma kinase (ALK) expression in the inflammatory myofibroblastic tumor: A comparative immunohistochemical study. Am J Surg Pathol 25:1364–1371.

Cools J, Wlodarska I, Somers R, Mentens N, Pedeutour F, Maes B, De Wolf-Peeters C, Pauwels P, Hagemeijer A, and Marylen P (2002). Identification of novel partners of ALK, the anaplastic lymphoma kinase, in anaplastic lymphoma and inflammatory myofibroblastic tumor. Genes Chromosomes Cancer 34:354–362.

Davidson E, Caffarella J, Vitseva O, Hou YM, and King MP (2001). Isolation of two cDNAs encoding functional human cysteinyl-tRNA synthetase. Biol Chem 382:399–406.

De Paepe P, Baens M, Van Krieken H, Verhasselt B, Stul M, Simons A, Poppe B, Laureys G, Brons P, Vandenberghe P, Speleman F, Praet M, De Wolf-Peeters C, Marylen P, and Wlodarska I (2003). ALK activation by the CTLC-ALK fusion is a recurrent event in large B-cell lymphoma. Blood, prepublished online, May 15.

Debelenko LV, Zhuang Z, Emmert-Buck MR, Chandrasekharappa SC, Manickam P, Guru SC, Marx SJ, Spiegel AM, Collins FS, Jensen RT, Liotta LA, and Lubensky IA (1997). Allelic delitions on chromosome 11q13 in multiple endocrine neoplasia type 1-associated and sporadic gastrinomas and pancreatic endocrine tumors. Cancer Res 57:2238–2243.

Dishop MK, Warner BW, Dehner LP, Kriss VM, Greenwood MF, Geil JD, and Moscow JA (2003). Successful treatment of inflammatory myofibroblastic tumor with malignant transformation by surgical resection and chemotherapy (2003). J Pediatr Hematol Oncol 25:153–158.

Donner LR, Tromple RA, and White RR 4th (1996). Progression of inflammatory myofibroblastic tumor (inflammatory pseudotumor) of soft tissue into sarcoma after several recurrences. Hum Pathol 27:1095–1098.

Gascoyne RD, Lamant L, Martin-Subero JI, Lestou VS, Harris NL, Muller-Hermelink HK, Seymour JF, Horsman DE, Auvigne I, Espinos E, Siebert R, and Delsol G (2003). ALK-positive diffuse large B-cell lymphoma is associated with Clathrin-ALK rearrangements: Report of six cases. Blood, prepublished online, May 22.

Griffin CA, Hawkins AL, Dvorak C, Henkle C, Ellingham T, and Perlman EJ (1999). Recurrent involvement of 2p23 in inflammatory myofibroblastic tumor. Cancer Res 59:2776–2780.

Hernandez L, Bea S, Bellosillo B, Pinyol M, Falini B, Carbone A, Ott G, Rosenwald A, Fernandez A, Pulford K, Mason D, Morris SW, Santos E, and Campo E (2002). Diversity of genomic breakpoints in TFG-ALK translocations in anaplastic large cell lymphomas: Identification of a new TFG-ALK(XL) chimeric gene with transforming activity. Am J Pathol 160: 1487–1494.

Hernandez L, Pinyol M, Hernandez S, Bea S, Pulford K, Rosenwald A, Lamant L, Falini B, Ott G, Mason DY, Delsol G, and Campo E (1999). TRK-fused gene (TFG) is a new partner of ALK in anaplastic large cell lymphoma producing two structurally different TFG-ALK translocations. Blood 94: 3265–3268.

Hu RJ, Lee MP, Connors TD, Johnson LA, Burn TC, Su K, Landes GM, and Feinberg AP (1997). A 2.5-Mb transcript map of a tumor-supressing subchromosomal transferable fragment from 11p15.5, and isolation and sequence analysis of three novel genes. Genomics 46:9–17.

Hussong JW, Brown M, Perkins SL, Dehner LP, and Coffin CM (1999). Comparison of DNA ploidy, histologic, and immunohistochemical findings with clinical outcome in inflammatory myofibroblastic tumors. Mod Pathol 12:279–286.

Kempson RL, Fletcher CDM, Evans HL, Hendrickson MR, and Sibley RK (2001). Tumors of the soft tissues. Rosai J, Sobin LH, editors. Washington, DC: Armed Forces Institute of Pathology, 83–86.

Lacoste-Collin L, Roux FE, Gomez-Brouchet A, Despeyroux ML, Uro-Coste E, Coindre JM, and Delisle MB (2003). Inflammatory myofibroblastic tumor: A spinal case with aggressive clinical course and ALK overexpression. Case report. J Neurosurg 98(Suppl 2):218–221.

Lamant L, Dastugue N, Pulford K, Delsol G, and Mariame B (1999). A new fusion gene *TPM3-ALK* in anaplastic large cell lymphoma created by a (1;2)(q25;p23) translocation. Blood 93:3088–3095.

Lamant L, Gascoyne RD, Duplantier MM, Armstrong F, Raghab A, Chhanabhai M, Rajcan-Separovic E, Raghab J, Delsol G, and Espinos E (2003). Non-muscle myosin heavy chain (MYH9): A new partner fused to ALK in anaplastic large cell lymphoma. Genes Chromosomes Cancer 37:427–432.

Lamant L, Pulford K, Bischof D, Morris SW, Mason DY, Delsol G, and Mariame B (2000). Expression of the ALK tyrosine kinase gene in neuroblastoma. Am J Pathol 156: 1711–1721.

Lawrence B, Perez-Atayde A, Hibbard MK, Rubin BP, Dal Cin P, Pinkus JL, Pincus GS, Xiao S, Yi ES, Fletcher CD, and Fletcher JA (2000). *TPM3-ALK* and *TPM4-ALK* oncogenes in inflammatory myofibroblastic tumors. Am J Pathol 157:377–384.

Ma Z, Hill DA, Collins MH, Morris SW, Sumegi J, Zhou M, Zuppan C, and Bridge JA (2003). Fusion of *ALK* to the Ran-binding protein 2 (*RANBP2*) gene in inflammatory myofibroblastic tumor. Genes Chromosomes Cancer 37:98–105.

Maes B, Vanhentenrijk V, Wlodarska I, Cools J, Peeters B, Marynen P, and de Wolf-Peeters C (2001). The *NPM-ALK* and *ATIC-ALK* fusion genes can be detected in non-neoplastic cells. Am J Pathol 158:2185–2193.

Meis JM and Enzinger FM (1991). Inflammatory fibrosarcoma of the mesentery and retroperitoneum: A tumor closely simulating inflammatory pseudotumor. Am J Pathol 15: 1146–1156.

Meis-Kindblom JM, Kjellstrom C, and Kindblom LG (1998). Inflammatory fibrosarcoma: Update, reappraisal, and perspective on its place in the spectrum of inflammatory myofibroblastic tumors. Semin Diagn Pathol 15:133–143.

Mitelman F (1995). ISCN: An International System for Human Cytogenetic Nomenclature. Mitelman F, editor. Basel: S. Karger, 1995.

Morris SW, Kirstein MN, Valentine MB, Dittmer KG, Shapiro DN, Saltman DI, and Look AT (1994). Fusion of a kinase gene, ALK, to a nucleolar protein gene, *NPM*, in non-Hodgkin's lymphoma. Science 263:1281–1284.

Morris SW, Xue L, Ma Z, and Kinney MC (2001). Alk+ CD30+ lymphomas: A distinct molecular genetic subtype of non-Hodgkin's lymphoma. Br J Haematol 113:275–295.

Pettinato G, Manievel JC, De Rosa N, and Dehner LP (1990). Inflammatory myofibroblastic tumor (plasma cell granuloma). Clinicopathologic study of 20 cases with immunohistichemical and ultrastructural observations. Am J Clin Pathol 94:538–546.

Popenko VI, Cherny NE, Beresten SF, Ivanova JL, Filonenko VV, and Kisselev LL (1993). Immunoelectron microscopic location of tryptophanyl-tRNA synthetase in mammalian, prokaryotic and archaebacterial cells. Eur J Cell Biol 62:248–258.

Reid LH, Davies C, Cooper PR, Crider-Miller SJ, Sait SN, Nowak NJ, Evans G, Stanbridge EJ, deJong P, Shows TB, Weissman BE, and Higgins MJ (1997). A 1-Mb physical map and PAC contig of the imprinted domain in 11p15.5 that contains TAPA1 and BWSCR1/WT regions. Genomics 43: 366–375.

Rodrigues GA and Park M (1994). Oncogenic activation of tyrosine kinases. Curr Opin Genet Dev 4:15–24.

Siebert R, Gesk S, Harder L, Steinemann D, Grote W, Schlegelberger B, Tiemann M, Wlodarska I, and Schemmel V (1999). Complex variant translocation t(1;2) with TPM3-ALK fusion due to cryptic *ALK* gene rearrangement in anaplastic large-cell lymphoma. Blood 94:3614–3617.

Sirvent N, Hawkins AL, Moeglin D, Coindre JM, Kurzenne JY, Michiels JF, Barcelo G, Turc-Carel C, Griffin CA, and Pedeutour F (2001). ALK probe rearrangement in a t(2;11;2)(p23; p15;q31) translocation found in a prenatal myofibroblastic fibrous lesion: Towards a molecular definition of an inflammatory myofibroblastic tumor family? Genes Chromosomes Cancer 31:85–90.

Snyder CS, Dell'Aquila M, Haghighi P, Baergen RN, Suh YK, and Yi ES (1995). Clonal changes in inflammatory pseudotumor of the lung: A case report. Cancer 76:1545–1549.

Spencer H (1984). The pulmonary plasma cell/histiocytoma complex. Histopathology 8:903–916.

Su LD, Atayde-Perez A, Sheldon S, Fletcher JA, and Weiss SW (1998). Inflammatory myofibroblastic tumor: Cytogenetic evidence supporting clonal origin. Mod Pathol 11:364–368.

Tort F, Pinyol M, Pulford K, Roncador G, Hernandez L, Nayach I, Kluin-Nelemans HC, Kluin P, Touriol C, Delsol G, Mason D, and Campo E (2001). Molecular characterization of a new ALK translocation involving moesin (MSN-ALK) in anaplastic large cell lymphoma. Lab Invest Mar 81:419–426.

Treissman SP, Gillis DA, Lee CL, Giacomantonio M, and Resch L (1994). Omental-mesenteric inflammatory pseudotumor. Cytogenetic demonstration of genetic changes and monoclonality in one tumor. Cancer 73:1433–1437.

Trojan A, Stallmach T, Kollias S, and Pestalozzi BC (2001). Inflammatory myofibroblastic tumor with CNS involvement. Onkologie 24:368–372.